Investigation of Scaling Laws by Critical Neutron Scattering from Beta-Brass

J. ALS-NIELSEN
The Danish Atomic Energy Commission, Research Establishment Risö, Roskilde, Denmark
(Received 4 April 1969)

Using a Cu^{65}-Zn β-brass crystal, the critical scattering of neutrons has been studied, both above and below T_c. The staggered susceptibilities χ vary as $C_+(T/T_c-1)^{-\gamma}$ and $C_-(1-T/T_c)^{-\gamma'}$, respectively. We find that $\gamma=\gamma'$ within an accuracy of 3%, in agreement with the scaling hypothesis of static critical phenomena; and that $C_+/C_-=5.46\pm0.05$, in excellent agreement with the recent parametric representation theory of Schofield and in fair agreement with the results of series expansions by Essam and Hunter. For fixed q, a flat maximum is observed in the wave-vector-dependent susceptibility $\chi(q, T)$ at temperatures which agree well with the predictions of Fisher and Burford.

IN theoretical investigations of phase transitions, the Ising magnet has been studied extensively because it is the simplest model which displays the essential features of critical phenomena. Only very few magnetic materials can be described adequately by the Ising model, so the possibilities for experimental verification of the theories may appear to be rather limited. However, the configurational energy in an AB alloy such as β-brass is formally equivalent to the Ising Hamiltonian, and, indeed, our previous investigations of the order-disorder transition in β-brass[1] have provided some accurate verifications of the theoretical predictions for the Ising model.[2]

The critical scattering cross section is proportional to the wave-vector-dependent susceptibility $\chi(\mathbf{q},t)$, where $\mathbf{q}$ is the difference between the scattering vector and a point in reciprocal space with an odd sum of indices, e.g., (1,0,0). The temperature dependence of the susceptibility is given in terms of $t=|T-T_c|/T_c$. We have, in particular, been interested in determining the temperature dependence of $\chi(0,t)$ above and below T_c, in order to compare the critical exponents γ and γ' given by:

$$\chi_+(0,t_+)=C_+t_+^{-\gamma}, \quad \chi_-(0,t_-)=C_-t_-^{-\gamma'}. \tag{1}$$

The indices + and − indicate temperatures above and below T_c, respectively. The scaling hypothesis of static critical phenomena implies $\gamma=\gamma'$.[3]

The long-range-order Bragg scattering occurring below T_c obscures the critical scattering for $\mathbf{q}$ near zero, so $\chi_-(0,t_-)$ can only be determined by correctly extrapolating the data for $\mathbf{q}\neq0$. The low critical scattering intensity in the region with no Bragg scattering contamination has previously prevented accurate determination of the susceptibility below T_c. However, the cross section is enhanced by a factor of 7 in a β-brass crystal isotopically enriched in Cu^{65}. We have produced a Cu^{65}-Zn crystal of 100 g, and the results described are derived from this crystal.

Unfortunately, although the q dependence of $\chi_+(\mathbf{q},t)$ has been calculated very accurately,[2] theoretical knowledge of $\chi_-(\mathbf{q},t)$ is very limited, so the optimum method of extrapolating to $q=0$ must be determined empirically. An appropriate expansion of $\chi(\mathbf{q},t)$ for small q/κ is

$$\chi_\pm(q,t_+)=\chi_\pm(0,t_\pm)/[1+b_\pm(q/\kappa_\pm)^2+\cdots]. \tag{2}$$

κ is the true correlation range as defined by Fisher and Burford.[2] A similar expansion with $b=1$ defines the effective correlation range κ_1, and $b\equiv(\kappa/\kappa_1)^2$. In general, $b\neq1$, but for the bcc lattice $b_+\simeq1$. The temperature dependence of κ near T_c is given by:

$$\kappa_+=F_+t_+^{\nu}, \quad \kappa_-=F_-t_-^{\nu'}. \tag{3}$$

For a fixed q, we may calculate the ratio of the temperatures t_+' and t_-' for which $\chi_+(q,t_+')=\chi_-(q,t_-')$. For small q, the leading term in an expansion of t_+'/t_-' will be the constant $(C_+/C_-)^{1/\gamma}$. The expansion to first order in $(\gamma'-\gamma)/\gamma$ and $(q/\kappa)^2$ is easily derived from (1)–(3):

$$\frac{t_+'}{t_-'}\simeq\left(\frac{C_+}{C_-}\right)^{1/\gamma}\left[1+\frac{\gamma-\gamma'}{\gamma}\ln t_-'-\frac{b_+}{\gamma}\left(\frac{q}{\kappa_+}\right)^2\epsilon\right], \tag{4}$$

with

$$\epsilon=1-b_-\kappa_+^2/b_+\kappa_-^2\simeq1-b_-F_+^2C_+/b_+F_-^2C_-. \tag{5}$$

We shall discuss the experimental data in terms of Eqs. (4) and (5).

In Fig. 1 the intensity of critical scattering in a temperature scan at fixed $q=0.04$ Å^{-1} is shown. The high-temperature data extending up to $t_+=0.035$ are not shown. Similar measurements were made at $q=0.02$ Å^{-1} and $q=0.06$ Å^{-1}. The intensities were corrected for Bragg scattering in the following way: The ratio $R(q)$ between Bragg scattering at wave vector q and $q=0$ was measured far below T_c, where the critical scattering is negligible. $R(q)$ was found to be independent of temperature in the interval $0.07<t_-<0.23$. Assuming that $R(q)$ remains constant up to the critical temperature, the Bragg scattering correction at a certain temperature is $R(q)$ times the Bragg peak

[1] J. Als-Nielsen and O. W. Dietrich, Phys. Rev. **153**, 706 (1967); O. W. Dietrich and J. Als-Nielsen, *ibid.* **153**, 711 (1967); J. Als-Nielsen and O. W. Dietrich, *ibid.* **153**, 717 (1967).
[2] M. E. Fisher and R. Burford, Phys. Rev. **156**, 583 (1967).
[3] L. Kadanoff *et al.*, Rev. Mod. Phys. **39**, 395 (1967).

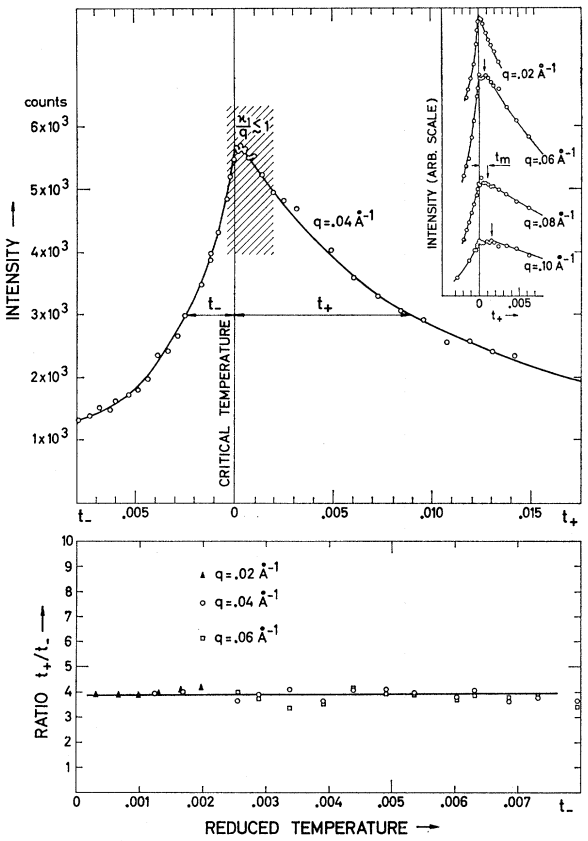

FIG. 1. Critical scattering intensities at fixed $q=0.04$ Å^{-1}. The ratio of equi-intensity temperatures outside the shaded region is constant, independent of q (lower part). Insert: The flat maximum above T_c is located near t_m, given theoretically by $\kappa^2(t_m)/q^2\simeq 0.023$.

intensity at that temperature. At $q=0.02$ Å^{-1}, one obtains $R(q)=0.18\%$, implying a 10% correction of the critical scattering at $t_-=0.002$. As the correction increased very rapidly for q below 0.02 Å^{-1}, it was not possible to determine $\chi_-(q,t)$ at smaller wave vectors.

We now consider the temperatures t_+ and t_- at which the scattered intensities above and below T_c are equal for a fixed value of $\mathbf{q}=\mathbf{q}_0$. The intensity at a spectrometer setting $\mathbf{q}_0$ is a folding of the cross section and the instrumental resolution. Therefore, it is not possible to conclude immediately that equal intensities correspond to equal cross sections $\chi_\pm(\mathbf{q}_0,t_\pm)$. However, if the intensities at t_- and t_+ are equal within a region in $\mathbf{q}$ space which is considerably greater than the extension of the resolution function, we may conclude unambiguously that $\chi_-(\mathbf{q}_0,t_-)=\chi_+(\mathbf{q}_0,t_+)$. Provided that $q_0<\kappa_+(t_+)$, the experimental data satisfy this condition and the ratio t_+/t_- is shown for various values of q_0 in the lower part of Fig. 1. Under these circumstances $t_+/t_-=t_+'/t_-'$ and, as the ratio is independent of q, the last term of Eq. (4) must be negligible.

[4] J. W. Essam and D. L. Hunter, Proc. Phys. Soc. (London) [J. Phys. **C1**, 392 (1968)].

Since $(q/\kappa_+)^2$ varies from about 1 to less than 0.01, this implies that ϵ must be of the order of 0.05 or less, i.e., $b_-\simeq(F_-/F_+)^2/(C_+/C_-)$. In the mean-field approximation $F_-/F_+=\sqrt{2}$ and $C_+/C_-=2$. For the two-dimensional Ising magnet $F_-/F_+=2$ and $C_+/C_-=37$. For the three-dimensional Ising magnet $C_+/C_-=5.1$,[4] and we estimate that $F_+/F_-\simeq 1.6$–1.8. This estimate and the experimental result that $\epsilon\simeq 0$ indicate that $b_-\simeq 0.4$–0.7, i.e., there is probably a rather large difference between the true and the effective correlation ranges below T_c.

The difference between γ and γ' can now be found from the variation of t_+/t_- with t_-. With a conservative estimate of systematic errors, we conclude from the data in the lower part in Fig. 1 that

$$(\gamma-\gamma')/\gamma=0.01\pm 0.02.$$

This result is significant in providing the first accurate experimental evidence for that aspect of the scaling hypothesis which implies $\gamma=\gamma'$. A weighted average of t_+/t_- yields

$$C_+/C_-=5.46\pm 0.05.$$

This result can be compared to the parametric representation theory of the equation of state by Schofield[5] which implies that $C_+/C_-=[(1-2\beta)^\gamma/2(\gamma-1)\beta]^{\gamma-1}\gamma/\beta$. Here β is the critical exponent for the magnetization near T_c. Inserting the experimental values for β and γ [1] gives $C_+/C_-=5.5$, whereas the theoretical values for β and γ give $C_+/C_-=5.3$. The value for C_+/C_- has also been determined from the series expansions of Essam and Hunter[4]; they find $C_+/C_-=5.1$ for the bcc Ising magnet.

The data for small values of t_+ display a flat maximum at $t_+=t_m$, and t_m increases with increasing q, as seen from the insert of Fig. 1. The occurrence of a flat maximum above T_c was anticipated by Fisher and Burford.[2] They predicted that t_m is determined by $\kappa_+^2(t_+=t_m)/q^2=0.023$ for the bcc Ising model. The arrows in Fig. 1 indicate the theoretical values of t_m and the agreement with the experimental data is satisfactory.

It may be noted that a temperature shift of the maximum scattered intensity has been observed in Fe, Ni, and Co.[6–8] However, as pointed out by Kocinski and Mrygon,[9] an interpretation of these temperature shifts in terms of the theory of Fisher and Burford seems unjustified, since the observed shift in Fe is zero for $q\lesssim 0.10$ Å^{-1} and then increases as q^4. Furthermore, Stump and Springer (private communication) have found that the temperature shift in Ni depends strongly on the perfection of the crystal. We

[5] P. Schofield, Phys. Rev. Letters **22**, 606 (1969).
[6] K. Blinowski and R. Ciszewski, Phys. Letters **28A**, 389 (1968).
[7] N. Stump and G. Maier, Phys. Letters **12**, 625 (1967).
[8] D. Bally, B. Grabcev, M. Popovic, M. Totia, and A. A. Lungu, J. Appl. Phys. **39**, 459 (1968).
[9] J. Kocinski and B. Mrygon, Phys. Letters **28A**, 386 (1968).

believe, therefore, that the observed temperature shift in β-brass is the first relevant experimental evidence for the predictions of Fisher and Burford.

I am grateful to M. E. Fisher and A. R. Mackintosh for discussions on the interpretation of the reported experimental results, and to L. Passell of Brookhaven National Laboratory for help in procuring the separated Cu^{65} used in the crystal.

PHYSICAL REVIEW VOLUME 185, NUMBER 2 10 SEPTEMBER 1969

Nernst Effect and Flux Flow in Superconductors. III. Films of Tin and Indium*

V. A. Rowe and R. P. Huebener
Argonne National Laboratory, Argonne, Illinois 60439
(Received 21 April 1969)

Flux motion induced by a temperature gradient and by an electrical current has been studied through the Nernst effect and the flux-flow resistivity in superconducting films of tin and indium. The film thickness ranged between 1 and 11 μm for tin and between 0.5 and 5 μm for indium. The data were taken at 2.0 K as a function of magnetic field and film thickness. In addition to the transport entropy of a fluxoid and the flux-flow resistivity, the critical thermal force and the critical Lorentz force, at which thermally induced and current-induced flux motion sets in, were determined. The transport entropy per unit length per unit flux, S_φ/φ, plotted versus film thickness was found to reach a maximum in Sn at about 7 μm and in In at about 3.5 μm. Around this maximum, S_φ/φ was larger by a factor of 1.4 in Sn and 1.6 in In than the value calculated from the difference in entropy density of normal and superconducting material. With increasing film thickness, the critical Lorentz force decreased, while the critical thermal force increased. The discrepancy between the critical Lorentz force and the critical thermal force and its dependence on film thickness suggests that in the films the critical current flows along special channels at the surface for which the interaction with the fluxoids is strongly reduced. The results on Sn and In are consistent with the earlier results on Pb.

I. INTRODUCTION

RECENTLY we reported measurements of the Nernst effect in the mixed state of superconducting niobium[1] and in the intermediate state of superconducting lead films.[2] In this paper we present the results of an extension of these measurements to superconducting films of tin and indium. The results obtained are similar to those reported in II for lead.

A summary of the theory and the scheme used for the analysis of the data can be found in I. Some of the experimental techniques described in I and II have been modified for the present work. Those parts of the experimental procedures which have been modified are described in Sec. II.

II. EXPERIMENTAL

The samples for these experiments were prepared by vacuum deposition of 99.9999% pure material[3] on 1-mm-thick microscope slides that had been cut to $1\frac{1}{2}\times\frac{13}{16}$ in. to fit the cryostat. The starting pressure in the bell jar was $\sim 5\times 10^{-8}$ Torr. During evaporation the pressure was in the 10^{-6}-Torr range for all samples except In 24 and In 26, for which the pressures were each an order of magnitude higher. The distance between the joule-heated tantalum boat and the sample substrates was 31 cm. With the exception of the two mentioned above, all samples were masked by a copper foil prepared by a photographic-reduction-and-etching process, thus giving a relative precision of sample dimensions of about $\frac{1}{2}$%. Substrates were cleaned first in detergent, then in an ultrasonic cleaner and finally in a vapor degreaser operating with trichloroethylene.

Film thickness d was measured routinely by the weight and the electrical resistance and checked occasionally by multiple-beam interferometry. The three methods were in good agreement for all the samples. Table I shows dimensions and residual-resistance ratios ($RRR=R_{295}/R_{4.2}$) of all the films except the In films of thickness greater than 3 μm, where the Nernst voltages were negligibly small. The sample configuration is shown schematically in Fig. 1. Number 36 Teflon insulated niobium lead wires were soldered to

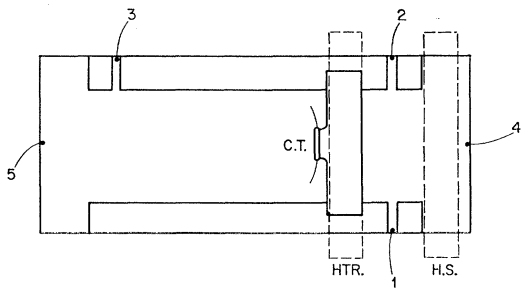

FIG. 1. Specimen geometry, including the heater (HTR), heat sink (HS), carbon thermometer (CT), Nernst probes (1 and 2) longitudinal voltage probes (2 and 3), and current leads (4 and 5).

* Based on work performed under the auspices of the U. S. Atomic Energy Commission.
[1] R. P. Huebener and A. Seher, Phys. Rev. 181, 701 (1969) (hereafter referred to as I).
[2] R. P. Huebener and A. Seher, Phys. Rev. 181, 710 (1969) (hereafter referred to as II).
[3] Source: Semi-Elements, Inc., Saxonburg, Pa. 16056.